JOURNAL OF MATERIALS SCIENCE 28 (1993) 3879–3884

Analysis of surface roughness using confocal microscopy

D. A. LANGE, H. M. JENNINGS, S. P. SHAH
NSF Center for Advanced Cement-Based Materials, Department of Civil Engineering, Northwestern University, Evanston, IL 60208, USA

Confocal microscopy provides a convenient means of acquiring three-dimensional descriptions of objects. A new technique exploits the capability of confocal microscopy to quantify rough surfaces. The microscope "optically" sections the surface, and a computer transforms a series of sections into digital images and a topographic map. Using a straightforward algorithm, the computer analyses the topographic map to derive a roughness parameter that characterizes the texture of the surface.

1. Introduction

Roughness of surfaces is of interest to a wide range of researchers in materials science [1, 2]. A number of methods can be used to measure roughness and the selection of method often depends upon the desired resolution. For instance, roughness on an atomic scale might be best measured by an atomic force microscope while the roughness of a mountain range may be measured by a stereophotography technique. In the range of resolution of optical microscopy, a relatively new technique has become available.

Confocal microscopes are optical microscopes which have the unique capability of creating a bright image of the in-focus region of the specimen while causing all out-of-focus regions to appear dark. One of the major limitations of optical microscopy is an inherent narrow depth of field. However, by using a confocal microscope to assemble a series of optical sections, each taken at a different focal plane, a "through-focus" image can be created which has "infinite" depth of field. This ability to overcome the limitation of a narrow depth of field has allowed the confocal microscope to find a unique role in imaging non-flat or translucent specimens [3].

Through the construction of an image from a series of optical sections taken of a rough surface, confocal microscopy also has the ability to create topographic maps. The topographic map is a digital image in which each pixel is assigned a value that represents the z-level. Each pixel may be thought of as an x–y–z coordinate in the three-dimensional surface. The actual surface area of the specimen can be estimated by geometric construction of the surface represented by the topographic map. Once surface area is computed, roughness of the surface can be characterized.

2. Specimen preparation

Six specimens, shown in Fig. 1, were examined in this study [4]. Portland cement pastes and mortars containing two types of sand: a fine sand having a mean diameter of 150 μm and a coarse-grained sand having a mean diameter of 750 μm. In both cases, the sands have a narrow particle-size distribution and may be modelled as mono-sized spheres. All of the specimens had a water–cement ratio of 0.40 by weight. The pastes varied by their content of silica fume (mean diameter of about 0.15 μm) as an additive. In one case, 5% of the cement was substituted by silica fume, and in the other case, 10% of the cement was substituted by silica fume.

A Noran Instruments TSM Confocal Microscope was used throughout the experiment. The equipment, illustrated in Fig. 2, included an image analysis system which was used to manipulate the images and compute roughness parameters from the topographic maps. The best confocal images are achieved when the surfaces are of uniform colour and reflectivity. Because some of the specimens incorporated translucent silica sand, the fracture surfaces made opaque by gold-coating in a manner similar to that used to prepare a specimen for an SEM.

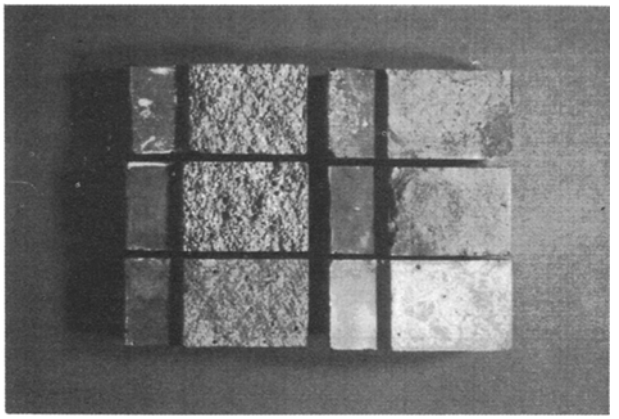

Figure 1 Gold-coated fracture surfaces of six specimens. Top left, coarse mortar 1:1; middle left, coarse mortar 1:2; bottom left, fine mortar 1:1; top right, 10% silica fume paste; middle right, 5% silica fume paste; bottom right, control paste.

0022–2461

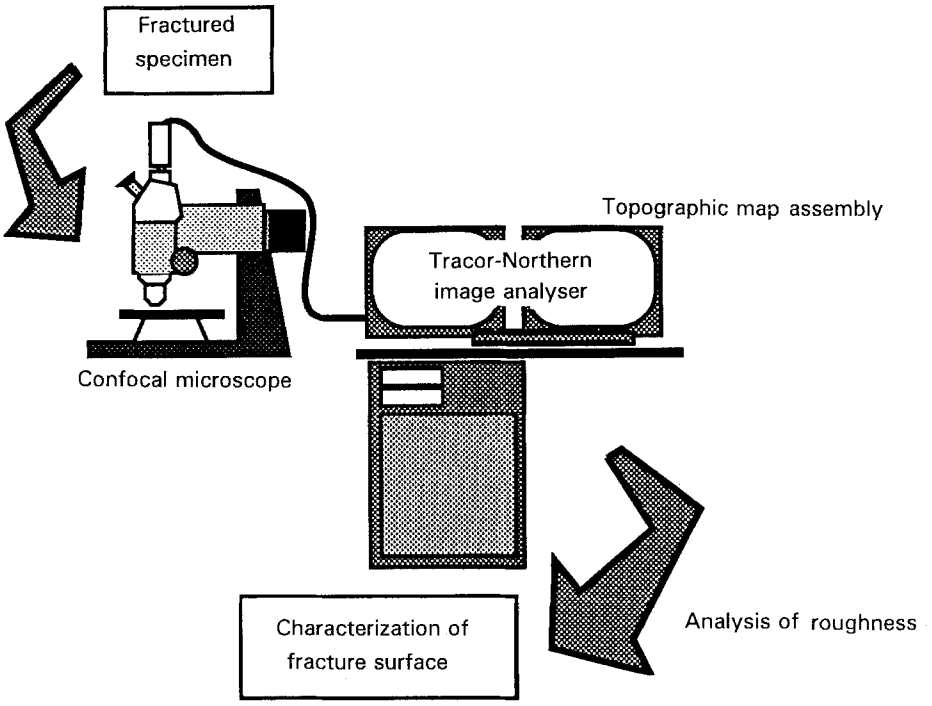

Figure 2 Confocal microscope and image analyser apparatus.

Material properties were evaluated by a comprehensive programme which included three-point bend tests of notched beams. The fracture surfaces resulting from the bend tests were observed by confocal microscopy as described below.

3. Construction of the topographic map

A typical image observed using the confocal microscope is shown in Fig. 3. The image is a grey image in which a full range of brightness is present. The bright areas correspond to in-focus regions; the dark areas are out-of-focus regions.

A topographic map is created by assembling a series of optical sections as illustrated in Fig. 4. As shown in Fig. 5, the intensity of a given pixel in the digital image will vary from section to section as the image goes in and out of focus. Every pixel (i.e. x–y coordinate) in the topographic map is assigned a numerical value that corresponds to the z-level of the section at which the pixel intensity is maximized.

The topographic maps are constructed using the algorithm described by the flow diagram in Fig. 6.

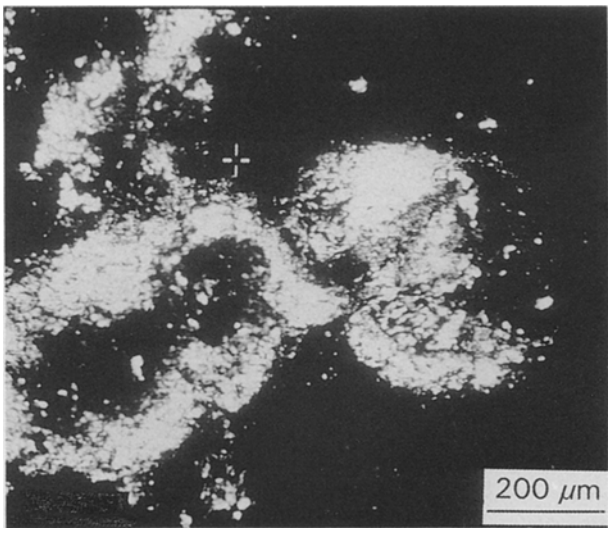

Figure 3 Typical image observed in confocal microscope.

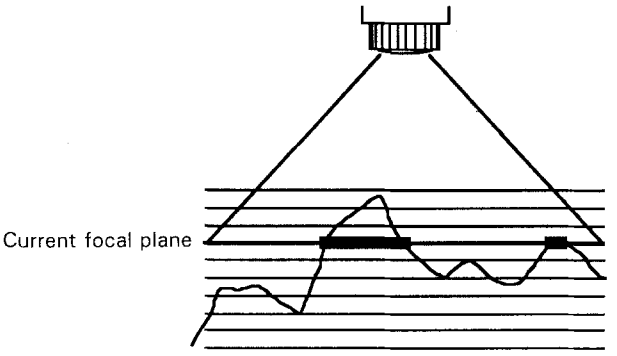

Figure 4 Optical sectioning with the confocal microscope.

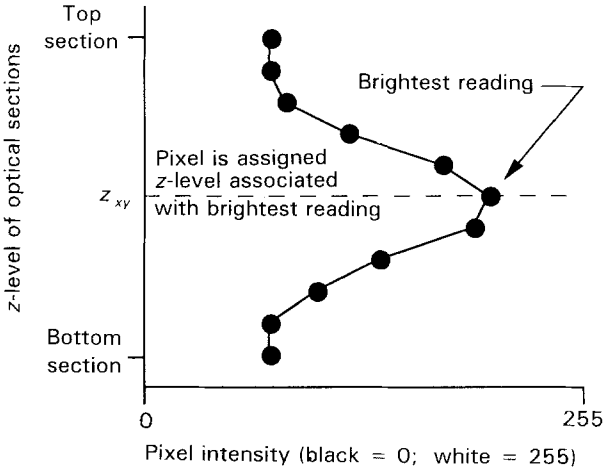

Figure 5 Typical pixel intensity as function of optical section z-level.

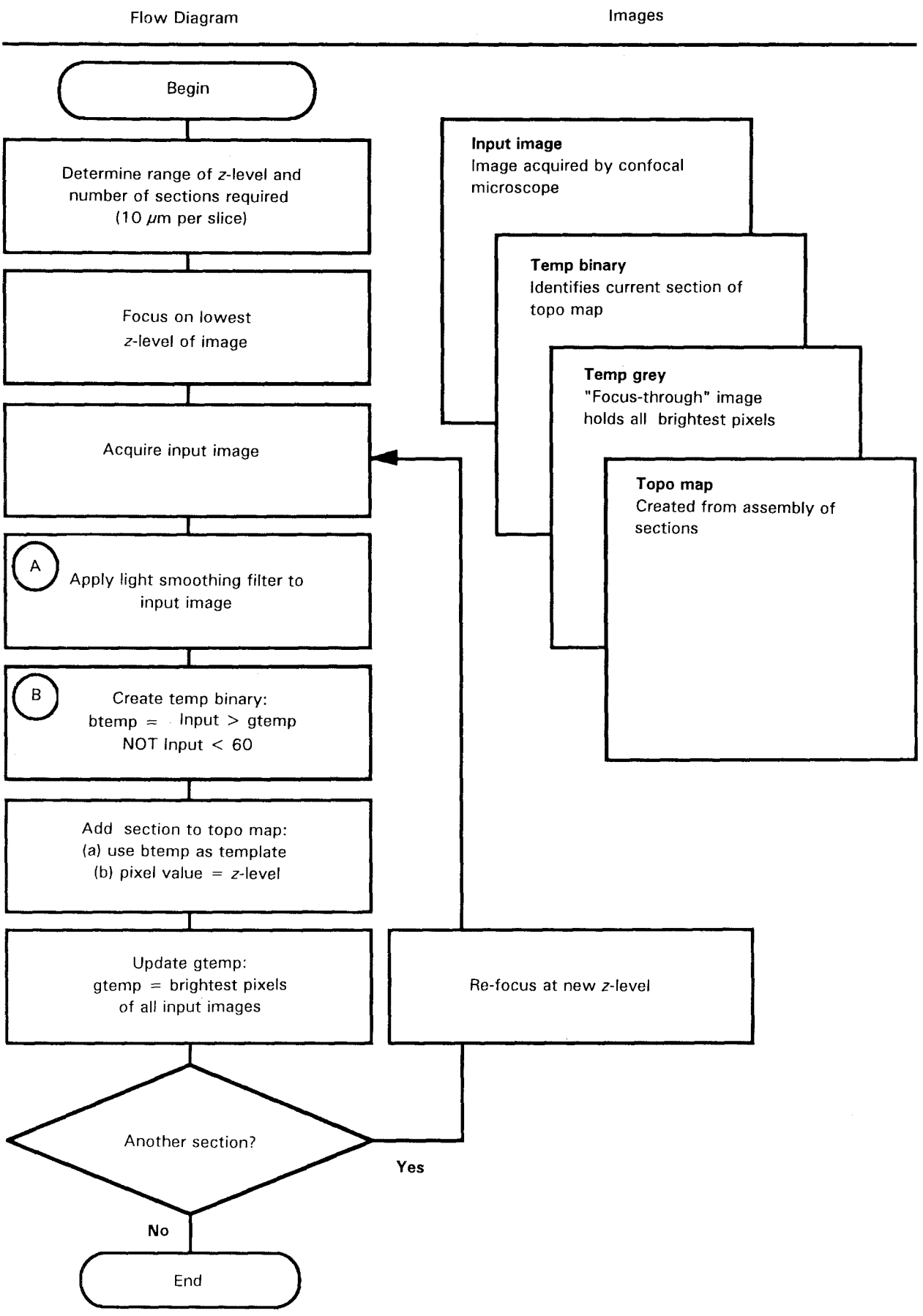

Figure 6 Flow chart for construction of topographic maps.

Initially, the range of z required to cover the visible fracture surface is determined by the operator. The number of optical sections (i.e. slices) is determined by dividing the range of z by the increment between slices. Throughout these experiments, 10 μm was used as the increment between slices. It is important to note that increment size *does* affect the computed roughness of the map. Preliminary experiments using a magnifica-

tion of ×90 showed that 10 μm was an appropriate increment to capture roughness of both paste and mortar in a meaningful way while not requiring an excessive number of slices to construct the maps. At a magnification of ×90, the field width was about 1 mm, and each pixel measured about 2 μm in width. The x–y resolution is controlled by magnification and the z resolution is controlled by slice thickness. While it is not necessary that x–y resolution and z resolution be equivalent, it is important to consider that both measures of resolution contribute to spatial resolution in the topographic map.

Four image buffers were used during the construction of a map. First, the raw image (referred to as input image) is acquired for each z-level. Second, the temporary grey image (referred to as temp grey or gtemp) is a record of the maximum intensity measured at each pixel as the series of optical sections is acquired. This image is also called a "through-focus" image because at the end of the acquisition of all slices, gtemp appears to be in focus at all depths. By itself, gtemp is useful to researchers interested in acquiring a through-focus image of a specimen that is too rough to fall within the normal depth of field. Third, a binary image buffer (referred to as temp binary or btemp) is used to identify the region of the image associated with a specific z-level. And fourth, a topo map buffer is required to hold the topographic map itself during the construction process. The topo map is not a grey image in the conventional sense of being composed of pixels ranging from 0–255. Rather, the pixel values of topo map record z-level, and may have any value. In the experiments described here, the range of z-level varied from about 200 μm for paste specimens to over 800 μm for images of mortar surfaces.

A light smoothing filter (Step A, Fig. 6) is applied to the raw image acquired at each z-level. The purpose of this light smoothing (i.e. averaging) is to diminish noise in the image. The degree of smoothing will affect the value of the roughness number. If no smoothing is used, noise during image acquisition results in a roughness number that is high. If heavy smoothing is used the maps appear unrealistically smooth. Although selection of an appropriate level of smoothing is a somewhat subjective decision, the important point is that the acquisition procedure and image processing must be the same for all specimens in order to have comparable results.

After smoothing, a binary is created to identify regions that may belong to the current z-level (Step B, Fig. 6). This binary is created by comparing the current image with the gtemp image buffer which holds the maximum intensity for each pixel in the image. It was also determined that a low threshold should be imposed in order to screen off dark regions of the acquired images. Dark regions of the optical sections are susceptible to being assigned improper z-levels. Although these regions were generally less than 1% of the total image area, error from dark regions was found to have a significant impact on compound roughness. A threshold of 60 (on the scale from 0–255 with 0 being black) was selected in preliminary experiments. Pixels in the image that never rise above 60 on any slice, will appear as "black holes" on the topographic map, and will be ignored in subsequent roughness measurement.

The binary buffer represents the area of the image associated with the current z-level. A slice is added to the topo map buffer by assigning the current z-level value to the pixels which are "on" in the binary image. The "off" pixels in the binary image are not changed from their previous value in the topo map.

In the end, each pixel in the topo map carries a value associated with the z-level at which it appeared brightest. This map can be visualized as a coloured two-dimensional contour map or as a three-dimensional rendering.

4. Computation of roughness number

A straightforward algorithm allows the confocal microscope to be used in a new way as a means to quantify roughness. The algorithm approximates the surface area of a topographic map by calculating the surface area of elements defined by four adjacent pixels, and then summing the surface elements over the entire image. A roughness number, R_S, is computed from the following equation

$$R_S = \frac{\text{actual surface area}}{\text{projected surface area}} \quad (1)$$

Plane geometry is used to find the surface area of each element. A representative element of area is illustrated in Fig. 7. The z-levels of four adjacent pixels are shown as z_1, z_2, z_3, and z_4. The line segments between points are shown as $s_{12}, s_{23}, s_{34}, s_{41}$, and s_{13}. The line segments create the sides of two triangles for which areas can be computed. The sum of the two triangular areas provides an approximation of the actual surface bounded by the four adjacent pixels. The equations used for this procedure are explained below.

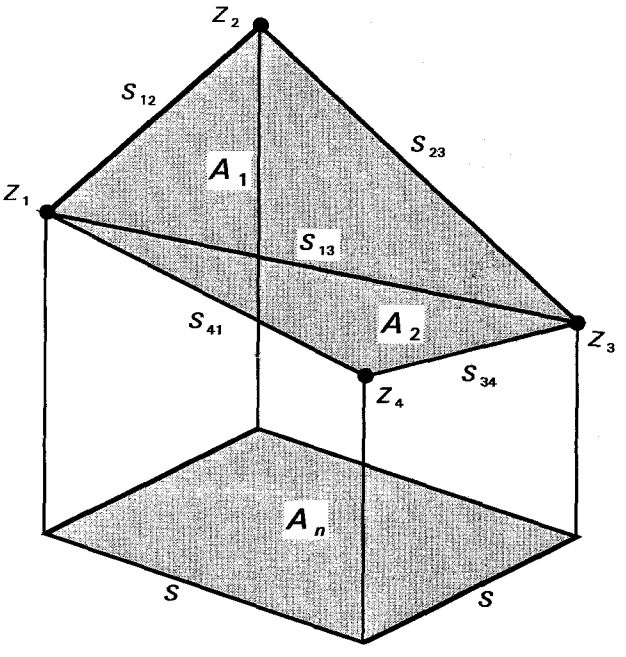

Figure 7 Representative area element bounded by four neighbouring pixels in the topographic map.

Line segments are given by

$$s_{ij} = [s^2 + (z_i - z_j)^2]^{1/2} \quad (2a)$$

except for s_{13} which is

$$s_{13} = [2s^2 + (z_1 - z_3)^2]^{1/2} \quad (2b)$$

Triangle perimeters are given by

$$2p_1 = s_{12} + s_{23} + s_{13} \quad (3a)$$

and

$$2p_2 = s_{34} + s_{41} + s_{13} \quad (3b)$$

Triangular areas are given by

$$A_1 = [p_1(p_1 - s_{12})(p_1 - s_{23})(p_1 - s_{13})]^{1/2} \quad (4a)$$

and

$$A_2 = [p_2(p_2 - s_{34})(p_2 - s_{41})(p_2 - s_{13})]^{1/2} \quad (4b)$$

Actual surface area is given by

$$A_S = A_1 + A_2 \quad (5)$$

Nominal surface area is given by

$$A_n = s^2 \quad (6)$$

Roughness parameter is given by

$$R_S = \frac{\text{actual surface area}}{\text{nominal surface area}} = \frac{\Sigma A_s}{\Sigma A_n} \quad (7)$$

The computed area of a specific element may vary depending on whether the algorithm makes two triangles by connecting points z_1–z_2–z_3 and z_1–z_3–z_4 instead of z_1–z_2–z_4 and z_2–z_3–z_4. However, such differences may be neglected when summing over 250 000 elements in an image.

As mentioned earlier, "black holes" are ignored by the algorithm. Black holes are designated by setting pixel values to zero. When the algorithm encounters a pixel set to zero, the surface area of the current element is not included, nor is the attendant nominal surface area included in the computation of roughness.

5. Analysis of surface roughness

The topographic maps are useful by themselves to provide a qualitative feel for the rough nature of the fracture surfaces. Fig. 8 is a typical map of the fracture surface of cement paste and Fig. 9 is a three-dimensional rendering of that same map. However, a quantitative measure of roughness is desired to provide a basis for comparing surfaces of different materials.

The computed roughness of the six specimens at two ages are presented in Table I. The roughness number of each specimen is the average of six maps. The specimens were tested at seven and 28 days after casting, and the specimens were cured in a lime-saturated bath of water.

The confocal technique suggests that the fracture surface areas of cement pastes are about 1.8 times greater than the nominal surface areas, and the mortars range from 2.4–2.8 times greater than the nominal surface areas.

The confocal technique did not discern significant differences between the roughness of 7 and 28 day specimens of a given mix. Furthermore, the roughness of the control paste, 5% silica fume paste and 10%

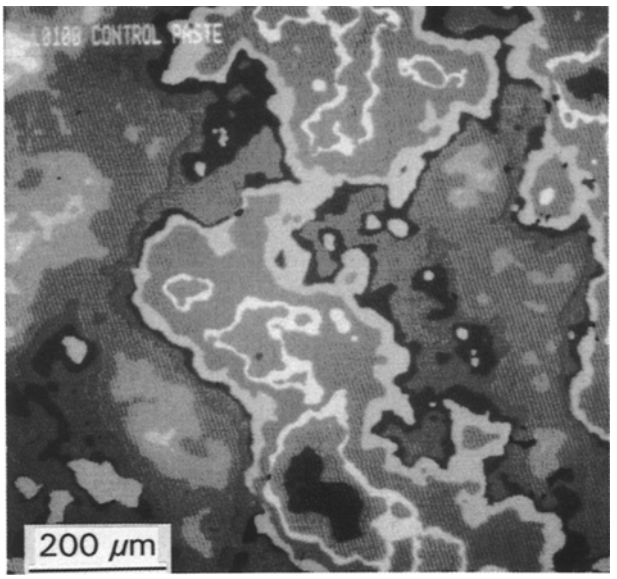

Figure 8 Two-dimensional representation of fracture surface of cement paste.

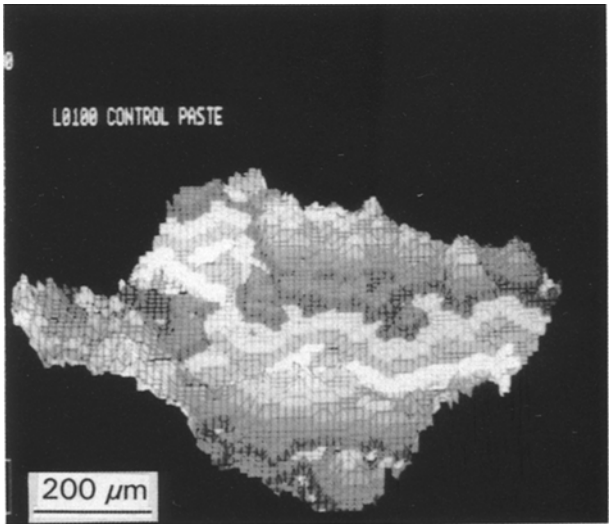

Figure 9 Three-dimensional rendering of fracture surface of cement paste.

TABLE I Roughness number, R_S, computed for all specimens

Specimen	7 day	28 day
10% silica fume paste	1.86	1.85
5% silica fume paste	1.78	1.85
Control paste	1.85	1.83
Coarse mortar 1:1	2.41	2.36
Fine mortar 1:1	2.42	2.53
Coarse mortar 1:2	2.79	2.78

silica fume paste were about the same. Visual inspection of all the control paste and silica fume paste specimens supports the finding that little difference is observed.

There are, however, notable differences in surface texture between the pastes and mortars, differences that are easily seen by visual inspection. These differences were quantified by the confocal technique.

Aggregate size is an important factor in fracture behaviour because the crack path tends to propagate through the matrix rather than through the aggregate. However, the results suggest that roughness of the fracture surface is not a simple function of largest aggregate size. Although both specimens incorporate the same aggregate, the coarse mortar 1:2 with high aggregate volume fraction (0.65) has a rougher fracture surface than the coarse mortar 1:1 with low aggregate volume fraction (0.48). Furthermore, the fine mortar 1:1 fracture surface has about the same roughness as the coarse mortar 1:1 even though the fine sand is one-fifth the diameter of the coarse sand.

6. Conclusions

The roughness of fracture surfaces have been characterized by a new technique using confocal microscopy. The fracture surface area of cement pastes are about 1.8 times greater than the nominal surface areas, and the mortars range from 2.4–2.8 times greater than the nominal surface areas. This finding has significant implications for fracture mechanics models of cement-based materials. The relationship between fracture energy and fracture surface texture of quasi-brittle materials such as cement and mortar is not a simple one. However, quantification of the three-dimensional tortuousity of the crack path may lead to a better understanding of the crack arresting/blunting mechanisms that absorb energy, and a more robust treatment of the micro-mechanics of fracture.

Acknowledgements

This research was supported by the NSF Center for Advanced Cement-Based Materials, Evanston, IL (Grant DMR-8808432-01) and equipment provided by the National Cement and Ceramics Laboratory, Evanston, IL.

References

1. E. E. UNDERWOOD, in "Proceedings of the 7th International Conference on Fracture", edited by K. Salama (Pergamon Press, Oxford, 1989) p. 3391.
2. J. C. RUSS, *JOM*, October (1990) 16.
3. B. YATCHMENOFF and R. D. COMPTON, *Ceram. Bull.* **69** (1990) 1307.
4. D. A. LANGE, PhD dissertation, Northwestern University, Evanston, IL (1991).

Received 27 April
and accepted 24 September 1992